IEEE Access
Multidisciplinary | Rapid Review | Open Access Journal

Date of publication February 02, 2023, date of current version February 02, 2023.

Digital Object Identifier 10.1109/ACCESS.2023.3244572

Optimal Capacitor Placement and Rating for Large-Scale Utility Power Distribution Systems Employing Load-Tap-Changing Transformer Control

EVAN S. JONES[1], (Student Member, IEEE), NICHOLAS JEWELL[1, 2], (Senior Member, IEEE), YUAN LIAO[3], (Senior Member, IEEE), and DAN M. IONEL[4], (Fellow, IEEE)

[1]Electrical and Computer Engineering Department, University of Kentucky, Lexington, KY, USA (e-mail: sevanjones@uky.edu)
[2]Louisville Gas and Electric and Kentucky Utilities, Louisville, KY, USA (e-mail: nicholas.jewell@lge-ku.com)
[3]Electrical and Computer Engineering Department, University of Kentucky, Lexington, KY, USA (e-mail: yuan.liao@uky.edu)
[4]Electrical and Computer Engineering Department, University of Kentucky, Lexington, KY, USA (e-mail: dan.ionel@ieee.org)

Corresponding author: Evan S. Jones (e-mail: sevanjones@uky.edu).

This work was supported by the Department of Education's GAANN Fellowship Program through the University of Kentucky Electrical and Computer Engineering Department. The support of Louisville Gas and Electric and Kentucky Utilities is also gratefully acknowledged.

ABSTRACT Significant opportunity for savings in energy and investment through improved performance of power distribution systems exists in the optimal placement and rating of capacitors, a conventionally cost-effective and popular reactive power compensating technology. A novel optimal capacitor planning (OCP) procedure is proposed for large-scale utility power distribution systems, which is exemplified on an existing utility circuit of approximately 4,000 buses. An initial sensitivity analysis is employed to intelligently reduce OCP computation time and maintain quality of optimal configurations. Three optimization objectives are considered, including the minimization of total system active power losses, standard deviation of node voltages, and investment in total capacitor power rating. Eight multi-objective optimization methods that employ the non-dominated sorting algorithm III (NSGA-III) concept are compared to determine individual merits. Differences between the methods include the incorporation of a penalty constraint for voltage violations and the automatic readjustment of load-tap-changing (LTC) transformer tap settings for proposed capacitor re-configurations concurrently within the optimizer, which ensures peak system performance and fair comparison to the reference case. A multi-step model conversion process was developed with OpenDSS to enable the OCP procedure to be generally applicable to real large-scale utility circuits. OCP is performed for three example sub-circuits served by a substation with a 48MW, 9Mvar peak load, which represents the most extreme case and offers the best opportunity for savings. Example configurations from the resulting Pareto sets through a pseudo-weight vector approach are also analyzed through a systematic procedure of comparison between the most extreme configuration types to inform configuration selection.

INDEX TERMS Capacitor, Control, Differential Evolution, Power Distribution Systems, OpenDSS, Optimization, Sensitivity Analysis, Load-Tap-Changing Transformers, Non-dominated Sorting Genetic Algorithm III

I. INTRODUCTION

CAPACITORS are typically employed in power distribution systems to increase system load capacity and overall power factor correction. This is achieved by providing voltage support and reactive power control functions, which also yields improved power losses and energy savings. Resulting harmonic effects and switching transients from control over time are considered secondary to the these main benefits.

Capacitor banks have long been considered a popular technology due to their lower cost and maintenance requirements when compared to other reactive power compensating devices. The traditional and currently most common method for capacitor installation relies on intuitive rules of thumb

supported by multiple powerflow studies to manually determine location and reactive power rating [1]. Such techniques can be arduous to perform and likely to provide sub-optimal solutions, especially for larger power distribution systems.

The yielded benefits of capacitors are directly determined by both their placement and rating [2]. Therefore, the application of an optimal capacitor planning (OCP) procedure, such as the one proposed in this work and illustrated in Fig. 1, offers the opportunity for improved savings and system performance. Such optimization is typically multi-objective in nature since costs from system power losses, capital investment, and voltage quality may compete.

A comparative study of multi-objective capacitor planning methods is presented, which includes novel approaches that may employ three concurrent objectives, a penalty constraint upon voltage violations during optimization, and the automatic adjustment of load-tap-changing (LTC) transformer tap settings to ensure peak system performance based upon proposed capacitor re-configurations. For the optimization algorithm, multi-objective versions of differential evolution (DE) and a genetic algorithm (GA) are considered and compared in performance and Pareto set quality. Optimal capacitor installation bus locations and ratings are simultaneously determined for three sub-circuits corresponding to transformers of a substation within a large 48MW, 9Mvar example power distribution system, which is made possible through an automated model conversion procedure of actual large-scale utility distribution systems.

The circuits are simulated at their peak loads since this scenario represents the most extreme condition of the circuit and the best opportunity for savings. Maximum load demand causes minimum voltage, and the most need is experienced for voltage support and reactive power compensation. With capacitors being switchable and becoming more easily controllable, those having been installed may be turned off for lower load situations to maintain operational compliance.

An initial sensitivity analysis is employed to improve computation time and maintain Pareto set quality, as the example real circuit is very large in scale with approximately 4,000 buses, which is a major contribution. A pseudo-weight vector approach is utilized to select optimal configurations based on provided weights, including the most extreme cases with respect to the considered objectives. A systematic procedure is proposed to analyze the extreme and existing reference configurations for each sub-circuit to inform configuration selection from among the corresponding Pareto sets.

In section II, a literature review is provided with primary focus upon existing capacitor planning methods that employ computational optimization. Section III establishes the power distribution system modeling and simulation procedure. Section IV formulates the capacitor planning problem and provides the sensitivity analysis for bus location installation candidacy, which corresponds to optimization decision variables. Considered optimization algorithms are explained in section V, and the methods which employ them are compared in section VI to establish their individual merits. Finally, a sub-circuit analysis to inform configuration selection is provided in section VII with conclusions in section VIII.

II. LITERATURE REVIEW

Upon review of relevant literature, special attention was placed on the selection of optimization objectives and algorithms employed in such studies. Additional constraints and the stage during which they were applied were also considered as well as example test power systems and modeling methods for both the networks and loads.

Proposed by A. Noori *et al.* is a hybrid allocation of capacitors and distributed static compensators in power distribution systems through multi-objective improved golden ratio optimization method (MOIGROM) and a fuzzy decision making process [3]. In this case, the MOIGROM has two objectives, including voltage violations and total installation cost corresponding to the equipment and related active power losses. A power loss reduction factor method is applied to determine buses most sensitive to reactive resource installation to reduce the decision variables considered by the MOIGROM. The procedure was applied to the IEEE 13, 69, and 118 bus test systems, resulting in solutions that improved both total active power losses and voltage violations on the example circuits.

Two optimal methodologies that both employ an epsilon multi-objective genetic algorithm ($\epsilon - MOGA$) for the allocation of both fixed and switching capacitors in a simulated real utility 162-bus power distribution network are explored by M. Ahmadi *et al.* [4]. Optimization objectives include minimization of total installation cost and switching frequency. The first method is a two-step process where installation location is determined by sensitivity analysis and the capacitor sizes by $\epsilon - MOGA$, whereas the second method utilizes $\epsilon - MOGA$ for both. The two-mechanism approach with an additional sensitivity analysis yielded better results, but both methods showed significant improvement in voltage profile, power losses, and financial investment.

Post-optimization constraints may also be applied as employed by Onaka *et al.* for the IEEE 34-bus test system to consider total harmonic distortion (THD) [5]. Optimal solutions are determined initially through the non-dominated sorting genetic algorithm II (NSGA-II) for two objectives in which the maximum bus voltage violations and total system costs considering capacitor installation as well as active power losses at both fundamental and harmonic frequencies are to be minimized. Solutions among the Pareto set, or optimal solution set of best compromise, that violate the THD constraint are removed from consideration.

Optimal placement and sizing of capacitors is determined by A. A. Eajal *et al.* for the IEEE 13-bus test system through a discrete particle swarm optimization (PSO) with a single objective of minimizing total system cost considering active power losses and capacitor installation [6]. A THD constraint is applied during the optimization instead of in the post-optimization stage as in [5].

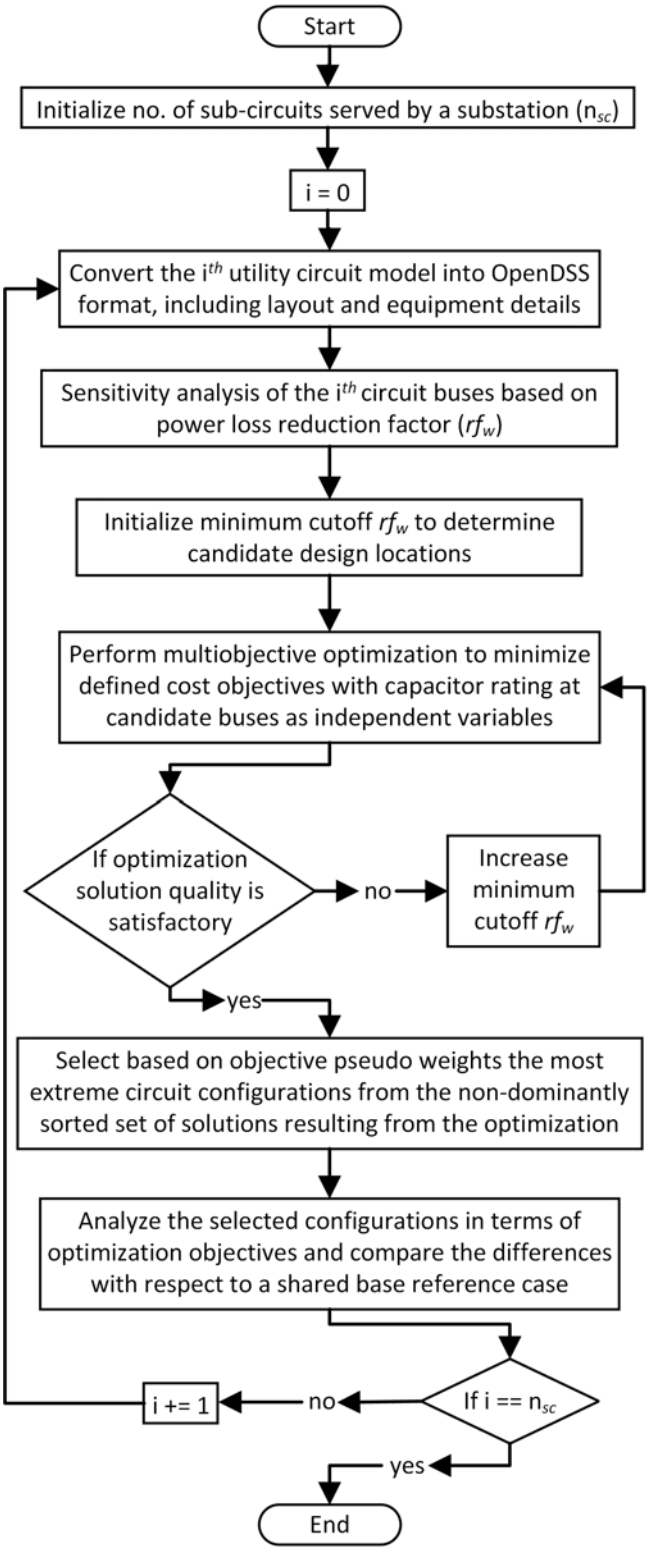

FIGURE 1. Flowchart for the overall proposed optimal capacitor planning (OCP) procedure with five main processes, including circuit modeling, candidate bus location determination, multi-objective optimization, solution selection considering objective priority, and selected configuration analysis.

An ant colony search optimization algorithm is proposed by C. F. Chang for both network reconfiguration and capacitor placement with the minimization of power losses as the only objective [7]. Voltage quality and other operating conditions are considering as constraints. It is also proposed that the method could be extended to automated control of distribution system devices over time.

Other optimization approaches have been applied to this capacitor placement and sizing problem, such as plant growth-based and multi-objective PSO or NSGA-II algorithms with differing objectives [8]–[15]. Some reported methods involve the hybrid utilization of different multi-criteria algorithms at different levels of a power system simulation, and comparisons of algorithm types have been provided [16]–[20].

It was found that typical objectives for capacitor planning generally include the minimization of active power losses and investment [3], [4], [6]. Constraints were also sometimes applied concurrently with the optimization or afterward upon the resulting Pareto set to ensure power system operational compliance for proposed capacitor configurations by limiting voltage violations and THD [5]–[7], [15].

The reconfiguration of other circuit elements to accommodate new capacitor arrangements has also been considered in literature, including by system topology alterations through changes in tie states and sectionalizing switches [21], [22]. Other studies have incorporated distributed generators (DGs) with their capacitor planning approaches, as renewable DGs like local solar PV are becoming more prevalent in modern power distribution systems [23]–[26].

Optimal capacitor planning for circuits with different load model scenarios have been studied [22], [27]–[29]. Such scenarios include different percentages of the peak load, variation in load based on customer types, or cases that model load voltage dependency. To study such cases on larger utility circuits, there is a need for enhanced load modeling methods with improved granularity, such as those that may employ data from advanced metering infrastructure (AMI) programs currently being deployed by utilities [30].

In addition to natural loadshapes, power distribution systems can experience considerable change in load demand and bus voltages due to operational events of typical control devices, such as LTC transformers and voltage regulators. A literature gap exists with respect to the readjustment of such devices upon reconfiguration of capacitors during the optimization process. LTC settings control the voltage profile of a power system and must be considered for a fair comparison to a base reference case.

Although comparative studies of optimization algorithms for OCP methods are available in current literature, the direct comparison of different methods in full, including their formulations, are insufficiently reported. The consideration or evaluation of capacitor efficacy over time as well as application of OCP on real large-scale power distribution systems are both limited in literature, as current studies usually only employ the IEEE test systems at their peak load instances.

The original contributions of this work are framed within the development and proposal of a novel OCP procedure (Fig. 1). These include a comparative study of multi-objective optimization approaches for a power system specific problem by employing computational intelligence methods and readjustment of LTC transformers, a new multi-step procedure for optimal power system configuration selection that utilizes a pseudo weight vector approach based on objective priority and a systematic analysis of the most extreme configuration types, and the application of OCP to three actual large-scale utility circuits, which was achieved through a custom-developed software to translate utility distribution system models into open-source OpenDSS versions for considerably improved accessibility.

III. POWER DISTRIBUTION SYSTEM MODELING AND SIMULATION

The example circuit, henceforth referred to as KUs1, utilized in the following study is a large 48MW, 9Mvar distribution system with advanced metering infrastructure (AMI) and is considered a candidate by its utility for implementing conservation voltage reduction (CVR) and volt-var optimization (VVO) programs (Fig. 2). KUs1 is significant in complexity, boasting 3,839 buses and 6,854 nodes, which serves approximately 5,000 homes in the U.S.

A software tool to convert power distribution system models from Synergi, a utility power system simulation software, to OpenDSS, an open-source software by the electric power research institute (EPRI), was developed with Python to enable the application of the OCP procedure on such circuits. This modeling procedure can also enable future CVR/VVO testing and benefit evaluation [31]–[34].

The KUs1 circuit OpenDSS model is a full copy of its Synergi counterpart which includes the matching of line mapping, impedances, and power losses, spot load demand, active and reactive powerflow, and bus voltages. Synergi requires two database files as input to produce circuit models, including the network and equipment files. The equipment file provides important parameters and descriptions of circuit components, such as cables, transformers, switches, and capacitors, typically employed by the utility. The network file describes the line mapping, component placement, peak load allocation, and operating details for the full circuit.

With the model conversion tool, circuit information is imported from the Synergi database input files and rewritten into OpenDSS format. To confirm accurate conversion, circuit model definitions and simulation results from both versions are compared at the global and individual component-level (Table I). Line lengths, positive and zero sequence components, and connection node mapping as well as the peak active and reactive powers of loads connected at each bus matched exactly. Simulated average voltages of the 3,839 buses yielded minimal percent difference with a mean of 0.17% and standard deviation of 2.65%.

Additional software for OCP has also been developed with Python by directly interfacing with the OpenDSS open-source software to employ as the modeling and simulation engine (Fig. 1). This tool set is utilized for the simulation of KUs1 at the peak load time instance for OCP and may be employed for time series simulation based upon a provided loadshape.

TABLE I. Global circuit conversion summary

	Active power [MW]	Reactive power [Mvar]	Losses [Mw]
Synergi	47.67	9.39	0.55
OpenDSS	47.90	9.94	0.50
Absolute diff.	0.23	0.55	0.05
(relative diff.)	(0.48%)	(5.86%)	(9.09%)

Such accurate circuit modeling and the prospective incorporation of AMI data to improve granularity in load modeling offers improved evaluation accuracy of effects from optimal planning and control. As an alternative to AMI, advanced load modeling through energy simulation of buildings and weather-dependant appliances is also of consideration [35]–[39].

IV. CAPACITOR PLANNING PROBLEM FORMULATION AND SENSITIVITY ANALYSIS FOR CANDIDATE INSTALLATION BUSES

Multi-objective optimization for OCP is proposed to determine the Pareto set of optimal capacitor configurations at the peak load instance. Two formulations are considered, each with four optimization method variations, resulting in eight sets of results for the example T1 sub-circuit of KUs1, which corresponds to a single transformer (Table II). An analysis is performed and provided in section VI to establish the relative merits of each of the formulations and optimization methods in terms of resulting Pareto sets and possible configurations.

Both problem formulations consider the installed capacitor reactive power ratings [kvar] for candidate capacitor installation bus locations as independent variables, which are determined by a sensitivity analysis discussed later in this section (Fig. 3). They share the same discrete range of 0 to 1,200kvar in increments of 300kvar, which corresponds to typically available capacitor sizes at the distribution system level. Both placement and rating are optimized simultaneously through the inclusion of 0kvar as a rating option.

The common objectives for the two formulations are to minimize total active power losses ($w_{a,t}$) and investment, which is represented by total installed capacitor rating ($c_{r,t}$):

$$\min \left[w_{a,t} = \sum_{i=1}^{n_l} (w_{a,l,i}) + \sum_{j=1}^{n_t} (w_{a,x,j}) \right], \tag{1}$$

$$\min \left[c_{r,t} = \sum_{i=1}^{n_c} (v_{r,i}) \right], \tag{2}$$

where n_c is the total number of capacitors to be installed; $c_{r,i}$, the reactive power [kvar] rating of capacitor number i; n_l, the total number of lines; $w_{a,l,i}$, the active power losses

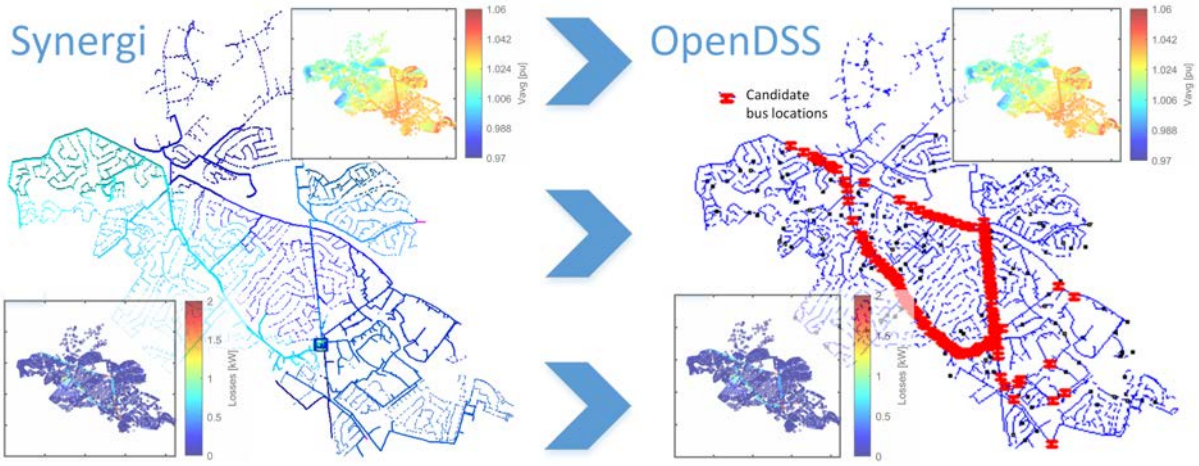

FIGURE 2. Comparison of the Synergi and converted OpenDSS circuit model line and component mappings for the original configuration of the actual 48MW, 9Mvar power distribution system KUs1. Also included for comparison are both individual bus voltage and line loss analyses for the peak load instance. The OpenDSS circuit diagram is labeled with the top candidate bus locations for capacitor installation. Candidacy is determined by a sensitivity analysis in terms of power loss reduction factor (rf_w) as discussed in section IV. Change in voltage for buses with high rf_w causes relatively significant change in power losses for connected lines. Such buses typically cluster near the main distribution feeder lines.

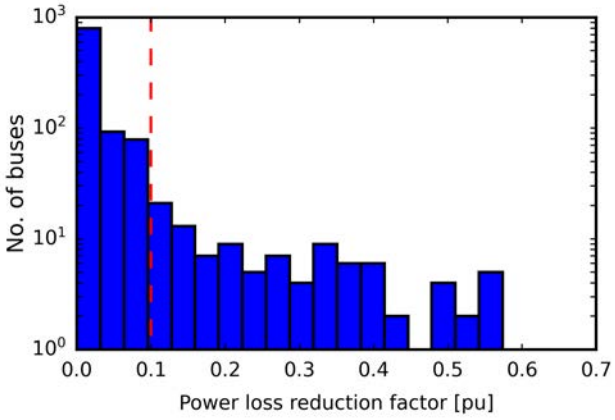

FIGURE 3. Histogram for rf_w of all buses in the KUs1 circuit with no. of occurrences on a logarithmic scale. Buses with higher rf_w correspond to those most sensitive to capacitor installation. The red line marks the minimum cutoff rf_w for consideration of candidacy.

[kW] at line number i; n_t, the total number of transformers; $w_{a,x,j}$, the active power losses [kW] at transformer number j; n_b, the total number of buses; v_i, the average voltage of all phases at bus number i; v_r, the reference voltage of 1.0pu.

For the second formulation, a third objective defined in equation (3) is proposed that minimizes the voltage variation throughout the circuit to improve distribution of capacitor installation locations and possibly reduce voltage violations over time, which is different from the typical approach that employs only two objectives. Lower voltage variation offers the prospect of reduced control operations and slower equipment degradation, which is being further explored in continued work. The function directly minimizes standard deviation of node voltages ($v_{n,d}$) and is defined as:

$$\min \left[v_{n,d} = \sqrt{\frac{\sum_{i=1}^{n_n} (v_{n,i} - v_{n,a})^2}{n_n}} \right], \tag{3}$$

where n_n is the total number of nodes in the circuit; $v_{n,i}$, the voltage at node number i; $v_{n,a}$, the mean voltage of all nodes.

To improve OCP performance and optimal configuration quality, a sensitivity analysis was performed to determine the best candidate bus locations for capacitor installation (Fig. 1). This effectively reduces the search space for the optimization algorithm and eliminates from consideration many buses that are not appropriate for capacitor installation. The analysis employed a power loss reduction factor (rf_w), defined as:

$$rf_w(i) = \frac{(\Delta w_i - \Delta w_{min})}{(\Delta w_{max} - \Delta w_{min})}, \tag{4}$$

where Δw_i, the difference in active power loss of the lines connected to bus i between two KUs1 simulation cases with transformer LTC tap settings set to 1.0pu and 1.05pu; w_{min}, the difference in minimum active power loss among the lines of the system; w_{max}, the difference in maximum active power loss among the lines on the system. rf_w captures the effectiveness of capacitor installation at a specific bus by determining the degree to which the change in active power losses of lines connected to the considered bus are dependent upon the change in voltage at that bus.

The list of candidate buses was further narrowed by excluding buses with fewer than three phases to comply with typical utility practices for capacitor installation. This effectively reduced the number of possible bus locations from approximately 4,000 to around 120. The bus candidate vector corresponds to the number of decision variables in the multi-objective optimization and directly relates to simulation time. This is important as future work with time series simulation

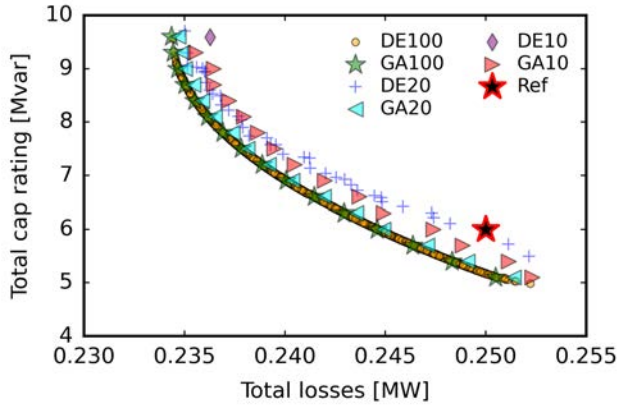

FIGURE 4. Comparison of resulting example Pareto sets for the KUs1 T1 sub-circuit from the most basic NM2 optimization employing the two considered optimization algorithms, NSDE (DE) and NSGA-III (GA), at different numbers of allowed generations as indicated legend labels.

will rely upon such an optimization to apply controls as the load changes.

V. OPTIMIZATION ALGORITHMS

For the OCP methods, two optimization algorithms are considered, including a non-dominated sorting differential evolution (NSDE) variant and the non-dominated sorting genetic algorithm 3 (NSGA-III) (Fig. 4). DE was originally designed for single-objective scalar optimization and has been adapted with a non-dominated sorting function to solve the OCP multi-objective problem due to its efficiency and effectiveness [40]. NSGA-III is an extension of the NSGA-II algorithm that is tailored to optimization problems that may have multiple objectives, which is innately suitable for OCP when coupled with a discrete independent variable set [41], [42].

Since typically available capacitor ratings are limited to larger units of 300kvar, an initial advantage of NSGA-III is the ability to employ a discrete independent variable set, whereas the NSDE variant may only utilize continuous variable ranges. This requires the NSDE method to incorporate an additional step to glean solutions with ratings that closely match what is actually available.

For initialization of the NSDE method, the configurations of selected ratings for the candidate installation bus locations within an initial population vector of the first generation are determined by use of uniform random number as follows:

$$PC_{g,p} = B_l + (B_u - B_l) * RAND_p(0,1), \qquad (5)$$

where g is the generation index and is equal to 1 to indicate the first generation; p, the population index and is equal to 1 to indicate the first population; B_u, the set of upper bounds; B_l, the set of lower bounds; $RAND_p(0,1)$, a function that produces a set of random values between 0 and 1 equal in size to population p.

Algorithm 1 Pseudo-code for the OCP optimization algorithm with continuous independent variable ranges based on the differential evolution concept.

Generate initial population vector $PC_{1,p}$
while termination criteria is not satisfied **do**
  for each population of power system configurations, p, in $PC_{g,p}$ **do**
    Generate permutation of random indices, R ▷ Mutation
    $PC_{M,g,p} \leftarrow PC_{g,p}[R[0]] + SF(PC_{g,p}[R[1]] - PC_{g,p}[R[2]])$
    if $RAND(0,1) \leq CR$ **then** ▷ Crossover
      $PC_{U,g,p} \leftarrow PC_{M,g,p}$
    else
      $PC_{U,g,p} \leftarrow PC_{g,p}$
    end if
    if $f(PC_{U,g,p}) \leq f(PC_{g,p})$ **then** ▷ Selection
      $PC_{g+1,p} \leftarrow PC_{U,g,p}$
    else
      $PC_{g+1,p} \leftarrow PC_{g,p}$
    end if
  end for
  $g \leftarrow g + 1$ ▷ Increment to next generation
end while

The configurations within the population $PC_{g,p}$ as defined in equation (5) are then mutated to create a new population ($PC_{M,g,p}$), which expands the search space:

$$PC_{M,g,p} = PC_{g,p} * R_0 + SF* \left[(PC_{g,p} * R_1) - (PC_{g,p} * R_2)\right], \qquad (6)$$

where R is a random permutation of distinct configurations and sf is a scaling factor that produces more population diversity as it is increased. sf is a positive value and is typically set within the range of [0,2] [40]. Based on the configurations from the target ($PC_{g,p}$) and mutated ($PC_{M,g,p}$) vectors, the cross-over procedure produces a population vector of trial configurations ($PC_{U,g,p}$) as follows:

$$PC_{U,g,p} = \begin{cases} PC_{M,g,p} & \text{if } RAND(0,1) \leq cr \\ PC_{g,p} & \text{otherwise} \end{cases} \qquad (7)$$

where cr is the cross-over probability. A random value for each of the individual configuration variables is generated as denoted by the $RAND(0,1)$ function. Finally, the selection step compares the evaluations of the objective function for $PC_{U,g,p}$ and $PC_{g,p}$ to improve or maintain the quality of $PC_{g,p}$ for the next generation, $PC_{g+1,p}$:

$$PC_{g+1,p} = \begin{cases} PC_{U,g,p} & \text{if } f(PC_{U,n,p}) \leq f(PC_{n,p}) \\ PC_{g,p} & \text{otherwise} \end{cases} \qquad (8)$$

This multi-step optimization procedure is repeated until

the termination criteria is satisfied. The Pareto set, or epsilon non-dominated sorted solution set of best compromise, is then determined as the set of optimal configurations.

Since this variant of DE is multi-objective, the process will terminate once a maximum number of generations is reached. This maximum value is determined by trial and comparison as illustrated in Fig. 4. The flow of the NSDE algorithm is further illustrated in Alg. 1. Sets included in Algs. 1 and 2 are indicated by their capitalization.

Algorithm 2 Pseudo-code for the OCP optimization algorithm with discrete independent variable ranges based on the concept of NSGA-III.

Randomly generate initial population vector of power system configurations $PC_{g,c}$ of size n_{pop} where g is generation number
Define a set of distributed reference points RP
$g \leftarrow 1$
while termination criteria is not satisfied **do**
  $PC_{g,S} \leftarrow \varnothing$, $i \leftarrow 1$
  $PC_{g,r} \leftarrow PC_{g,p} \cup PC_{g,c}$
  $F \leftarrow$ non dominated sorting of $PC_{g,r}$
  while $|PC_{g,S}| < N_{pop}$ **do**
    $PC_{g,S} \leftarrow PC_{g,S} \cup PC_{g,s}[i]$
    $i \leftarrow i + 1$
  end while
  $PC_{g,S} \leftarrow PC_{g,s}[i]$
  if $|PC_{g,S}| = N_{pop}$ **then**
    $PC_{g+1,p} \leftarrow PC_{g,S}$
    Criteria satisfied, break here
  else
    $P_{g+1,p} \leftarrow \cup_{j \leftarrow 1}^{l-1} PC_{g,s}[j]$
    Determine K number of points to be chosen from $PC_{g,s}$: $K \leftarrow N_{pop} - |P_{g+1}|$
    Normalize objectives
    Associate each member of $PC_{g,S}$ with a reference point $d \in H$
    Compute niche count of reference point j, where j is associated with member $k \in P_{g+1} \cap PC_{g,S}$
    Choose K members from $PC_{g,S}$ to construct P_{g+1}
  end if
  $g \leftarrow g + 1$ ▷ Increment generation
end while

Fundamentally, NSGA-II and NSGA-III follow the same process but with a different selection mechanism. In NSGA-II, new parent populations $PC_{g+1,p}$ are determined from a combined population $PC_{g,r}$, which is the union of the parent and child population sets ($PC_{g,p}$ and PCg, c, respectively) ordered by their rankings. Let the set $PC_{g,s}$ be the non-dominated sorting of $PC_{g,r}$. For each configuration, i, in a population of size n_{pop}, let the set $PC_{g,S}$ having been initialized as an empty set be the union of itself $PC_{g,S}$ and $PC_{g,s}[i]$. If the size of $PC_{g,S}$ becomes greater than n_{pop}, then only those members with the largest crowding distances among the last non-dominated front $PC_{g,s}$ are selected.

In NSGA-III, the best members from $PC_{g,s}$ are, instead, selected from the supplied reference points RP. In this work, the set RP was determined based on the Das and Dennis procedure [43]. Next, with $PC_{g,S}$ and RP, each objective's values are normalized based on $PC_{g,S}$. Then, references lines are constructed on a hyper-plane by joining the points of RP with the origin. The population members of $PC_{g,S}$ and $PC_{g,s}$ are then associated with a member of RP based on their closeness to the reference lines in the now normalized objective space.

The number of members from $PC_{g+1,p}$ that are in $PC_{g,S}$ which are associated with the members of RP are counted. If there is a reference point, or member of RP, that has no member associated with it and at least one of the members of $PC_{g,s}$ are associated with that member of RP, then the member of $PC_{g,s}$ with the shortest perpendicular distance to the corresponding reference line is added to PC_{g+1}. If all members of RP associate with at least one member of the population, then the member to be added to $PC_{g+1,p}$ is, instead, randomly selected from $PC_{g,s}$. This procedure, starting from the initialization of $PC_{g,S}$ inclusive, is repeated until a termination criteria, such as the desired population size or maximum number of generations, is satisfied. The flow of the NSGA-III algorithm is further illustrated in Alg. 2.

In comparing NSDE and NSGA-III at maximum generation numbers of 10, 20, and 100, it is evident that NSGA-III yields Pareto sets of better quality with fewer required generations than NSDE (Fig. 4). This is an additional advantage of NSGA-III, which already employs a discrete independent variable range that eliminates the need for removing configurations with invalid capacitor ratings as in the NSDE case with continuous ranges.

The proposed OCP procedure is being adapted in on-going work to act as an optimal control function, which would occur at each timestep of a simulation (Fig. 1). The number of required generations directly determines computation speed, as each generation requires the same amount of time and produces the same number of configurations in the design space. Although a practically identical Pareto set is reached by the optimization algorithms eventually, the computation speed is an important aspect in enabling real-time operation of the optimal control functionality. Therefore, all considered multi-objective OCP formulations in the following study employ NSGA-III.

VI. MULTI-OBJECTIVE OPTIMIZATION METHODS

For each of the the two problem formulations defined in section IV, four optimization methods are considered. The methods are compared based on results from the KUs1 T2 sub-circuit simulation. Corresponding merits are established in terms of Pareto set results and possible configurations. The differences in the four approaches include the incorporation of a penalty constraint for configurations with voltage violations and the method of adjusting the tap settings at the corresponding LTC transformer (Tab. II).

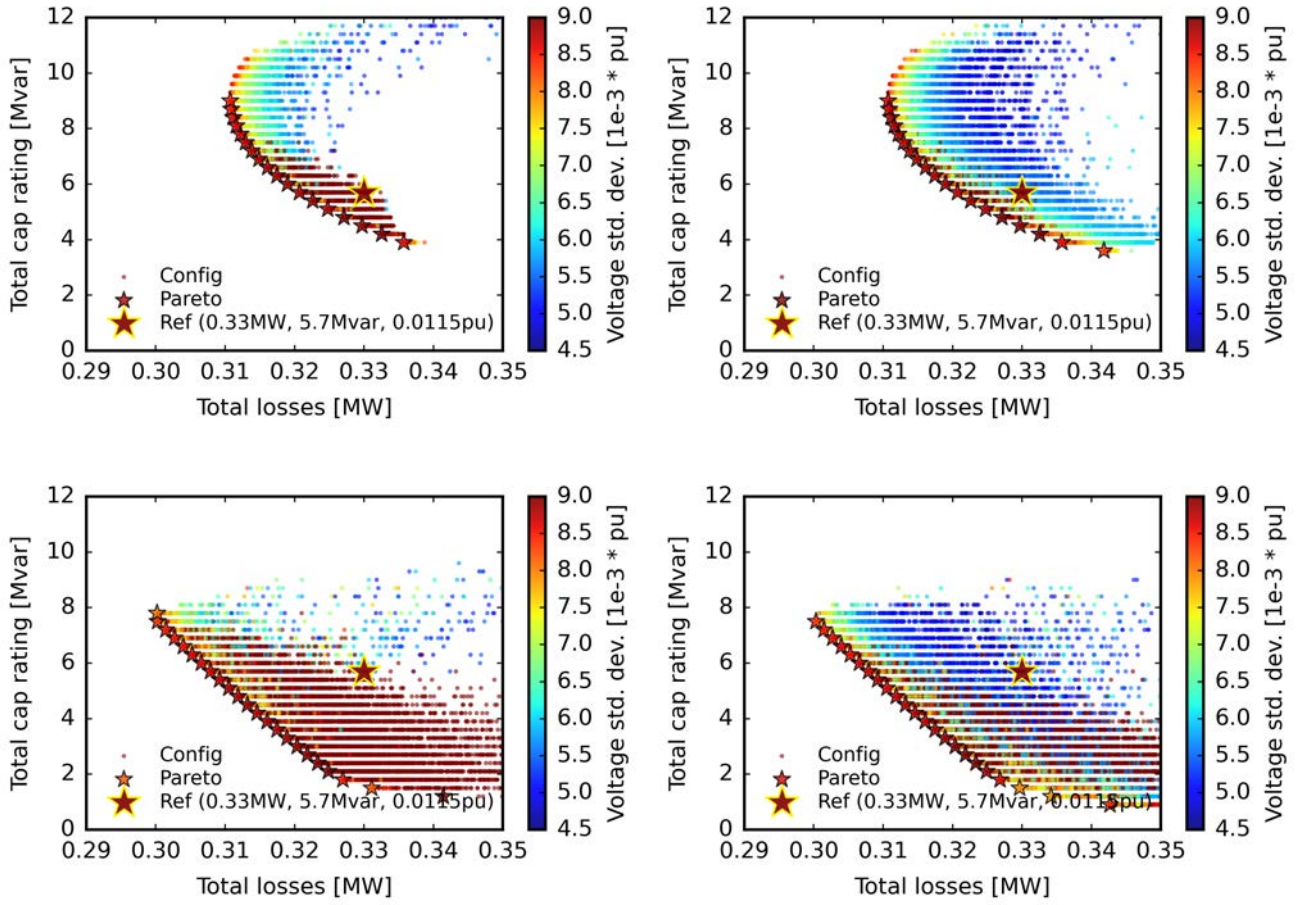

FIGURE 5. Possible configurations and Pareto sets for the (a) NM2, (b) PM2, (c) NA2, and (d) PA2 methods. Configurations with voltage violations of more than 0 are not considered and not illustrated within any of the plots. Introducing the penalty constraint as illustrated with PM2 and PA2 increases the breadth of the search space. It also provides additional valid configurations along the Pareto sets that require less investment. Incorporating automatic LTC tap setting adjustment within the optimizer, as in NA2 and PA2, improves overall $w_{a,t}$ and $c_{r,t}$.

TABLE II. Characteristics of the eight (8) considered optimization methods.

Optimization method	NM2	PM2	NA2	PA2	NM3	PM3	NA3	PA3
$w_{a,t}$ **objective**	Y	Y	Y	Y	Y	Y	Y	Y
$c_{r,t}$ **objective**	Y	Y	Y	Y	Y	Y	Y	Y
$v_{n,d}$ **objective**	N	N	N	N	Y	Y	Y	Y
Penalty constraint on voltage violations	N	Y	N	Y	N	Y	N	Y
Automatic LTC tap setting adjustment	N	N	Y	Y	N	N	Y	Y

The voltage violation penalty constraint is enacted by counting the the number of voltage violations experienced in each configuration considered by checking whether any nodes within the circuit have a voltage greater than 1.05pu or less than 0.95pu. When voltage violations are detected, $w_{a,t}$ is heavily penalized such that the configuration is no longer considered valid by the optimizer (Fig. 10).

For LTC transformer tap setting adjustment, two methods are considered. In the first, the LTC tap settings are manually adjusted in 1/32 increments, which corresponds to 32 possible settings, within a band of +/- 5% for the existing reference circuit such that bus voltages are as low as possible without causing any voltage violations (Fig, 10). Then, the tap settings are left unchanged for all configurations proposed by the optimizer.

Tap settings are determined and controlled by the optimizer in the second method so that power distribution system effects due to new capacitor configurations are considered concurrently. This is achieved by adding the tap settings as additional independent variables with a discrete range of 32 tap settings as applied in the manual adjustment technique.

The assigned optimization type names identify whether

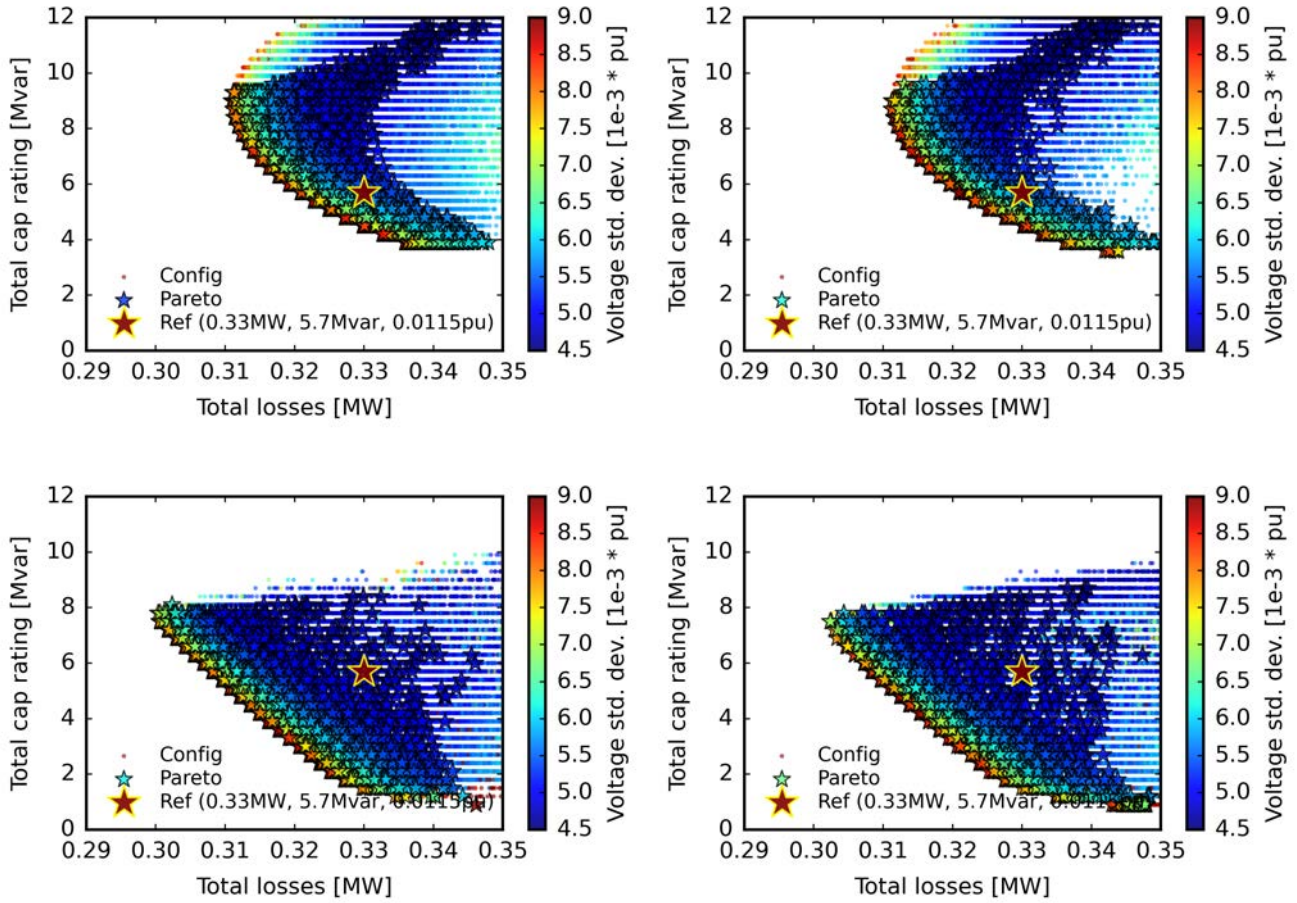

FIGURE 6. Possible configurations and Pareto sets for the three-objective (a) NM3, (b) PM3, (C) NA3, and (D) PA3 methods. Configurations with voltage violations of more than 0 are not considered and not illustrated within any of the plots. Effects observed in Fig. 5 remain present. The additional third objective increases focus by the optimizer in the region of increased $c_{r,t}$ and yields configurations with improved $v_{n,d}$, including some with penalty to $w_{a,t}$ and $c_{r,t}$, which indicates it's independence as a third objective.

the penalty constraint is employed (no penalty (N) or with penalty (P)) as well as the method of tap setting adjustment (manual, M, or automatic, A) and the number of objectives (2 or 3) considered (Table II). The most basic optimization method, NM2, yields an anticipated Pareto set of optimal capacitor configurations illustrated in Fig. 5a. Such configurations are favorable with respect to the reference case, which operates with relevantly average $c_{r,t}$.

For this case in the T2 sub-circuit, many options exist through which $w_{a,t}$ may be improved, even with reduced $c_{r,t}$. Configuration quality is very similar for PM2 as in NM2 with an expanded solution set throughout the lower region of reduced $c_{r,t}$, which is due to the penalty constraint against voltage violations (Fig. 5b). The expansion in search space by penalty constraint is also evident between NA2 and PA2 (Figs. 5c and 5d).

Introducing the automatic LTC transformer tap adjustment function in cases NA2 and PA2 considerably improves both the $w_{a,t}$ and $c_{r,t}$ across the set of possible solutions. Additionally, configurations of lower $c_{r,t}$ have especially improved $w_{a,t}$, as indicated by the steeper slope of the Pareto set (Fig. 7). Minimal $w_{a,t}$ is achieved by enabling the power system to operate at the highest voltage without violating standard limits. In the NA2 and PA2 cases, the optimizer is able to adjust the voltage of the entire system through LTC transformer tap control as well as increase the voltage of targeted nodes with particularly high rf_w.

The additional penalty constraint against voltage violations increases the size of the search space but more generally and without such focus in the lower $c_{r,t}$ region, especially for PA3 (Figs. 6 and 7). As anticipated, $v_{n,d}$ is mostly dependent upon capacitor placement with some correlation to increased $c_{r,t}$ since more capacitors are available to improve voltage uniformity. (Fig. 8).

The optimizer shifts in focus to the higher $c_{r,t}$ region for three-objective methods, since such optimal configurations can now also offer reduced $v_{n,d}$, sometimes with penalty to $w_{a,t}$. This adjusted focus is more so evident in methods NA3 and PA3, since configurations produced with these techniques can provide additional loss mitigation from higher tap

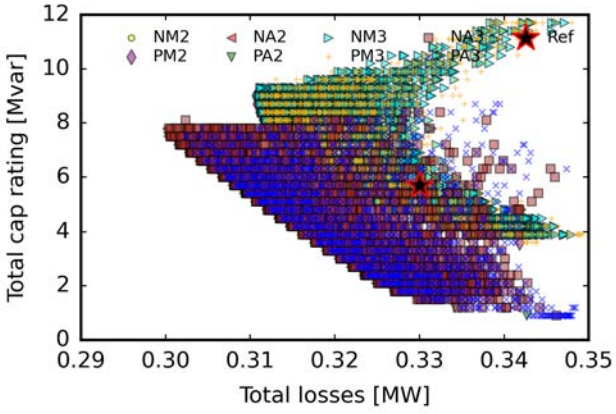

FIGURE 7. Pareto sets of $w_{a,t}$ and $c_{r,t}$ for all eight (8) optimization methods. The introduction of automatic LTC tap adjustment improves overall $w_{a,t}$ and $c_{r,t}$, especially for configurations of lower $c_{r,t}$.

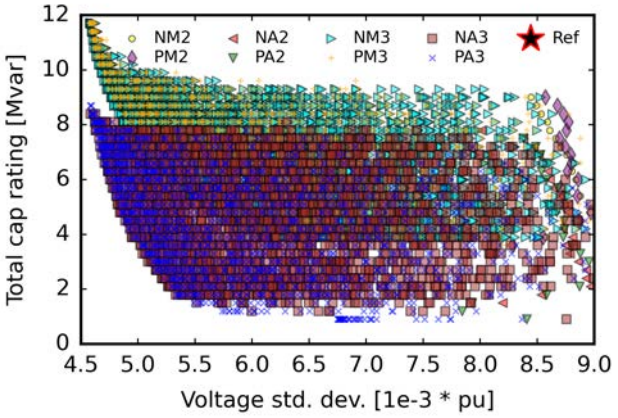

FIGURE 8. Pareto sets of $c_{r,t}$ and $v_{n,d}$ for all eight (8) optimization methods. $v_{n,d}$ is mostly dependent upon capacitor placement with some correlation to increased $c_{r,t}$ since more capacitors are available to improve voltage uniformity.

settings without voltage violations through improved voltage uniformity (Fig. 9).

Three-objective methods also provide additional configurations among the Pareto set with improved $v_{n,d}$ that do not necessarily correlate with the other two objectives. This contribution enables analysis of the trade-offs between all three without losing quality in configurations which focus more upon $w_{a,t}$ and $c_{r,t}$.

Study of these methodologies is ongoing and may be included in future publications. The implementation cost objective, which represents investment through total capacitor power rating, is being further developed as the total number of individual capacitors as well as their geographical location can also contribute.

Additionally, the application of these methodologies to capacitor switching and LTC settings for time-series optimal control of established devices is being considered to reduce total distribution system power by activating CVR and VVO functions without voltage violations. The evaluation of benefits yielded by these functions is enabled through ZIP parameter modeling of the distribution system loads to capture their voltage dependency. Advanced load modeling techniques, such as the incorporation of AMI data as it becomes more available from utilities, can improve the accuracy of such evaluation as it becomes more available in emerging smart grids [30].

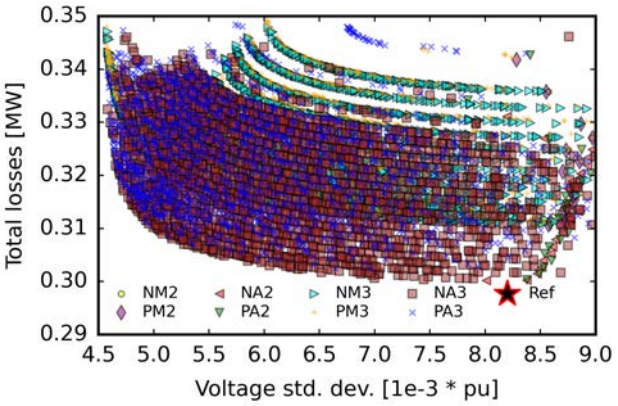

FIGURE 9. Pareto sets of $w_{a,t}$ and $v_{n,d}$ for all eight (8) optimization methods. Higher tap settings in the LTC tap function-enabled NA3 and PA3 methods further reduce $w_{a,t}$, which was made possible in part by improved $v_{n,d}$.

VII. OPTIMAL CONFIGURATION SELECTION THROUGH SUB-CIRCUIT ANALYSIS

The PA3 optimization technique was also applied to the other two sub-circuits of KUs1 (T1 and T3, Figs. 11 and 12). A decision-making procedure is proposed for configuration selection through the pseudo-weight vector approach [44]. Since the multi-objective optimization of PA3 minimizes three objectives, three weights with the requirement that they must sum to one are provided to the decision-making function to return a solution. For each solution s among the entire solution set S, this selection method calculates a pseudo weight for each objective obj by determining the normalized distance to the worst solution corresponding to each obj through the equation:

$$pw_{obj} = \frac{(f_{obj}^{max} - f_{obj}(s))/(f_{obj}^{max} - f_{obj}^{min})}{\sum_{n=1}^{N}[((f_n^{max} - f_n(s))/(f_n^{max} - f_n^{min})]} \quad (9)$$

where f_{obj}^{max} is the maximum result of obj among the solutions in S; $f_{obj}(s)$, the result of obj for s; f_{obj}^{min}, the minimum result of obj among the solutions in S; N, the set of objectives for each s of the set S; f_n^{max}, the maximum result of objective n for all of S; $f^n(s)$, the result of objective n for s; f_n^{min}, the minimum result of objective n for all of S.

Four unique circuit configuration types from among the Pareto sets of the three sub-circuits of KUs1 (T1, T2, and T3) were selected for comparison. The circuits are simulated at their respective peak load instances, and their reference

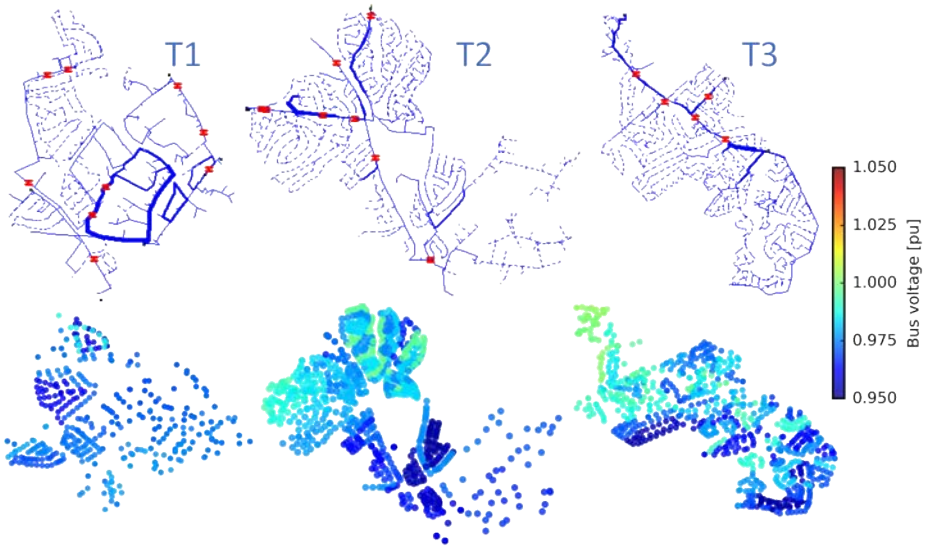

FIGURE 10. Circuit diagrams with reference capacitor locations and bus voltages for the KUs1 sub-circuits corresponding to substation transformers with tap settings such that voltages operate as low as possible without voltage violations.

capacitor configurations are provided as "Ref" (Fig. 10).

Among the selected solutions are the three most extreme cases with the objectives of $w_{a,t}$, $c_{r,t}$, and $v_{n,d}$, which are respectively defined in equations (1), (2), and (3), weighted at 100% and labeled as cases "W", "Q", and "D". The fourth configuration, "C", is an equal compromise of the objectives with weights of 33% each.

To further enable comparison of sub-circuits and capture compromise between objectives for the selected configurations in terms of improvement from the reference cases, compromise factors between the three objectives are proposed and calculated as follows:

$$cf_{w,q} = \left|\frac{\delta_w}{\delta_q}\right|, \quad cf_{d,q} = \left|\frac{\delta_d}{\delta_q}\right|, \quad cf_{w,d} = \left|\frac{\delta_w}{\delta_d}\right| \qquad (10)$$

where $cf_{w,q}$ is the compromise factor between active power losses ($w_{a,t}$) and total capacitor power rating ($c_{r,t}$); $cf_{d,q}$, between voltage standard deviation ($v_{n,d}$) and $c_{r,t}$; $cf_{w,d}$, between $w_{a,t}$ and $v_{n,d}$; δ_w, the absolute percent change in $w_{a,t}$ between the reference and selected configuration; δ_q, the absolute percent change in $c_{r,t}$; δ_d, the absolute percent change in $v_{n,d}$.

Among the three sub-circuits, T1 has exceptionally low δ_d across the selected configuration types and a low $cf_{d,q}$. This indicates that the base circuit excels in voltage uniformity regardless of capacitor configuration (Table III and Fig. 13). Such stable voltage along with higher $cf_{w,q}$ suggests that the compromise between $w_{a,t}$ and $c_{r,t}$ be of primary focus for configuration selection. Based on configuration Q, reducing the $c_{r,t}$ by 70% would yield a δ_w of only 15%. So, the capacitors in the T1 sub-circuit could be reconfigured with similar $w_{a,t}$ and $v_{n,d}$ with much less $c_{r,t}$.

For T2, δ_d has the most range with all configuration types, boasting reductions of up to 63% as well as very high values of $cf_{d,q}$. This indicates that the system is most sensitive to capacitor placement in terms of voltage variation (Fig. 14). Similar to T1, T2 could also be reconfigured with better δ_q, as much as -42%, at a small δ_w of up to 5%. The more favourable selection for T2 would considerably improve $v_{n,d}$ with a small penalty to $w_{a,t}$ at much lower $c_{r,t}$.

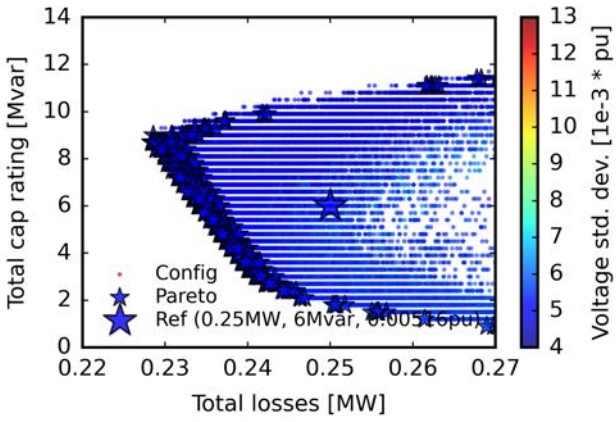

FIGURE 11. Possible configurations and Pareto set for T1. $v_{n,d}$ is exceptional for all configurations, including Ref, in comparison to T2 and T3. Improved $w_{a,t}$ is achieved with less $c_{r,t}$ with respect to Ref.

The T3 sub-circuit is different from T1 and T2 in that it requires considerably more $c_{r,t}$ to achieve similar improvements in $w_{a,t}$ and $v_{n,d}$. The W configuration offers the best δ_w of -10%, but at a high δ_q of 120% and with a very low $cf_{w,q}$ of 0.08. δ_q increases further to 210% for the D configuration, yielding a significant δ_d of -33% at a low $cf_{d,q}$ of 0.11. Therefore, reconfiguration of T3 based upon the corresponding Pareto set would require more $c_{r,t}$ of at least a 70% increase to begin realizing improved δ_w and δ_d as in T1 and T2.

TABLE III. Percent change to circuit characteristics applied by selected optimal configurations with respect to reference ("Ref") configuration and compromise factors as defined in Eq.10

Sub-circuit	**T1**				**T2**				**T3**			
Configuration	**C**	**W**	**Q**	**D**	**C**	**W**	**Q**	**D**	**C**	**W**	**Q**	**D**
δ_w	-2	-7	15	10	-2	-8	5	4	-7	-10	-3	-2
δ_q	40	30	-70	155	5	10	-42	90	130	120	70	210
δ_d	-3	-6	9	-11	-50	-36	-32	-63	-26	-21	-15	-33
$cf_{w,q}$	0.05	0.23	0.21	0.06	0.40	0.80	0.12	0.04	0.05	0.08	0.04	0.01
$cf_{d,q}$	0.08	0.20	0.13	0.07	10.00	3.60	0.76	0.70	0.20	0.18	0.21	0.11
$cf_{w,d}$	0.67	1.17	1.67	0.91	0.04	0.22	0.16	0.06	0.27	0.48	0.20	0.06

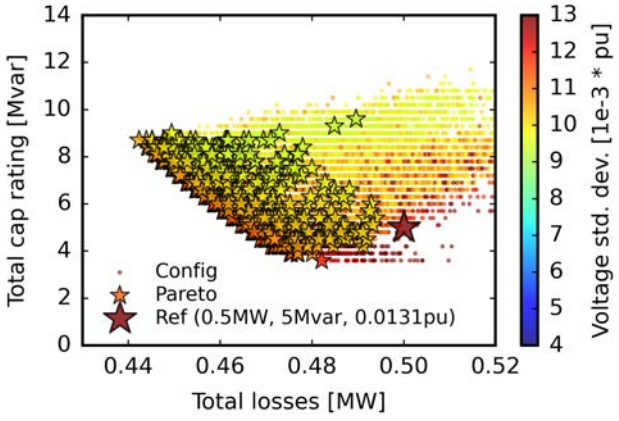

FIGURE 12. Possible configurations and Pareto set for T3. Considerable improvement of $v_{n,d}$ possible with reduced $c_{r,t}$ and $w_{a,t}$ compared to Ref.

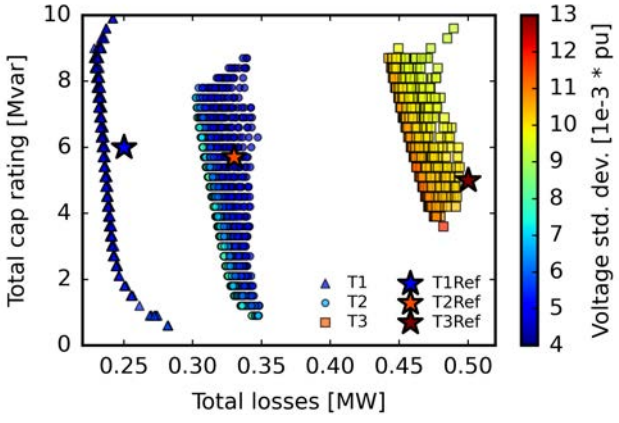

FIGURE 13. Comparison of the three Pareto sets with shared axes to illustrate how each sub-circuit may benefit from OCP with respect to their corresponding reference configurations and to each other in terms of the three objectives. T1 can experience similar $w_{a,t}$ with much less $c_{r,t}$ than Ref and no penalty to $v_{n,d}$. Opportunity exists for T2 and T3 to improve in $v_{n,d}$ with less $w_{a,t}$. T2 can achieve this with even less $c_{r,t}$ than Ref, whereas T3 would require more to yield similar benefits.

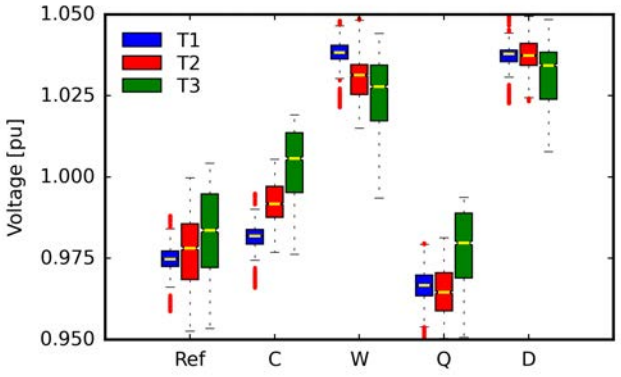

FIGURE 14. Circuit bus voltages of the three sub-circuits for each selected configuration type. As anticipated, D reduces $v_{n,d}$ more than the other configurations. Both T2 and T3 experience more $v_{n,d}$ than T1 and have the most opportunity for improvement in that regard.

VIII. CONCLUSIONS

Multi-objective optimization for capacitor placement and rating of large-scale utility circuits is achieved through a multi-step optimal capacitor planning (OCP) procedure developed through a comparison of methods, which include different formulations and optimization algorithms. The novel PA3 three-objective technique with both penalty constraint on voltage violations and automatic load-tap-changing (LTC) transformer tap setting adjustment was determined to be the most effective. A solution selection method through a pseudo-weight vector approach that considers objective priority was developed and employed to determine the three most extreme cases of the KUs1 sub-circuits as well as an even compromise configuration. The efficacy evaluation for capacitor configurations over time in addition to the peak load scenario may be enabled by future enhanced load modeling methods as utilities deploy advanced metering infrastructure (AMI).

Based on a systematic sub-circuit analysis of the selected configurations, significant improvements with respect to the base reference case were concluded. The T1 and T2 sub-circuits could be reconfigured to perform similar to the reference case with 70% and 42% less total installed capacitor rating, respectively. T2 was found to be most sensitive in voltage variation change and could be improved in this regard by up to 63%. T3 was unique in that the reference case had

a relatively low total installed capacitor rating and would require more investment to yield similar benefits in reduced power losses and voltage deviation as in T1 and T2.

ACKNOWLEDGMENT

This work was supported by the Department of Education's GAANN Fellowship Program through the University of Kentucky Electrical and Computer Engineering Department. The support of Louisville Gas and Electric and Kentucky Utilities, part of the PPL Corporation family of companies, is also gratefully acknowledged. Any opinions, findings, conclusions, or recommendations expressed in this material are those of the authors alone and do not necessarily reflect the views of the DoEd, LG&E and KU, or PPL.

APPENDIX

Included is a list of nomenclature for convenient reference.

NOMENCLATURE

VARIABLES

$w_{a,t}$	total active power losses
$c_{r,t}$	total installed capacitor rating
$c_{r,i}$	reactive power [kvar] rating of capacitor i
$w_{a,l,i}$	active power losses [kW] at line i
$w_{a,x,j}$	active power losses [kW] at transformer j
$v_{n,d}$	standard deviation of node voltages
v_i	average voltage of all phases at bus number i
$v_{n,i}$	voltage at node number i
$v_{n,a}$	mean voltage of all nodes
Δw_i	difference in active power loss of the lines connected to bus i between two cases with transformer LTC tap settings set to 1.0pu and 1.05pu
w_{min}	difference in minimum total active power loss
w_{max}	difference in maximum total active power loss
rf_w	variable that captures the effectiveness of capacitor installation at a specific bus by determining the degree to which the change in active power losses of lines connected to the considered bus are dependent upon voltage change
g	the generation index
p	the population index
sf	scaling factor
s	a solution from among the set S considered by the selection procedure
obj	indication of the objective with which a priority pseudo weight is associated
pw_{obj}	pseudo weight for objective obj
$cf_{w,q}$	the compromise factor between $w_{a,t}$ and $c_{r,t}$
$cf_{d,q}$	the compromise factor between $v_{n,d}$ and $c_{r,t}$
$cf_{w,d}$	the compromise factor between $w_{a,t}$ and $v_{n,d}$
δ_w	the absolute percent change in $w_{a,t}$ between the reference and selected configuration
δ_q	the absolute percent change in $c_{r,t}$ between the reference and selected configuration
δ_d	the absolute percent change in $v_{n,d}$ between the reference and selected configuration.

SETS

B_u	set of upper bounds
B_l	set of lower bounds
$PC_{g,p}$	target population set for generation g
$PC_{M,g,p}$	mutated population set for generation g
$PC_{U,g,p}$	population set after crossover for generation g
$PC_{g,p}$	parent population set during selection
PCg,c	child population set during selection
$PC_{g,r}$	population set produced by the union of $PC_{g,p}$ and PCg,c ordered by their rankings
$PC_{g,s}$	set $PC_{g,r}$ having been non-dominantly sorted
RP	set of reference points for NSGA-III
S	set of solutions considered by the selection
N	set of objectives for each s of the set S.

CONSTANTS

n_c	total number of capacitors to be installed
n_l	total number of lines
n_t	total number of transformers
n_b	total number of buses
v_r	reference voltage of 1.0pu
n_n	total number of nodes in the circuit
n_{sc}	total number of sub-circuits served by a substation
cr	cross-over probability
n_{pop}	set size of population in optimization procedure.

FUNCTIONS

$RAND_p(0,1)$	function that produces a set of random values between 0 and 1 equal in size to population p
f_{obj}^{max}	the maximum result of obj among the solutions in S
$f_{obj}(s)$	the result of obj for s
f_{obj}^{min}	the minimum result of obj among the solutions in S
f_n^{max}	the maximum result of objective n for all of S
$f^n(s)$	the result of objective n for s
f_n^{min}	the minimum result of objective n for all of S.

REFERENCES

[1] "Optimal Capacitor Placement: Costs Benefits Due to Loss Reductions," Operation Technology, Inc., 17 Goodyear, Irvine, CA 92618, Tech. Rep. [Online]. Available: https://etap.com/docs/default-source/white-papers/optimal-capacitor-placement-benefits.pdf?sfvrsn=9b37b27f_20

[2] H.-D. Chiang, J.-C. Wang, O. Cockings, and H.-D. Shin, "Optimal capacitor placements in distribution systems. i. a new formulation and the overall problem," *IEEE Transactions on Power Delivery*, vol. 5, no. 2, pp. 634–642, 1990.

[3] A. Noori, Y. Zhang, N. Nouri, and M. Hajivand, "Hybrid allocation of capacitor and distributed static compensator in radial distribution networks using multi-objective improved golden ratio optimization based on fuzzy decision making," *IEEE Access*, vol. 8, pp. 162 180–162 195, 2020.

[4] M. Ahmadi, M. S. S. Danish, M. E. Lotfy, A. Yona, Y.-Y. Hong, and T. Senjyu, "Multi-objective time-variant optimum automatic and fixed type of capacitor bank allocation considering minimization of switching steps," *AIMS Energy*, vol. 7, no. 6, pp. 792–818, 2019. [Online]. Available: https://www.aimspress.com/article/doi/10.3934/energy.2019.6.792

[5] J. H. D. Onaka, A. S. de Lima, A. R. A. Manito, U. H. Bezerra, M. E. L. Tostes, C. C. M. d. M. Carvalho, T. M. Soares, and D. C. Mendes, "Optimal capacitor banks placement in distribution grids using NSGA II and harmonic resonance chart," in *2016 17th International Conference on Harmonics and Quality of Power (ICHQP)*, 2016, pp. 89–94.

[6] A. A. Eajal and M. E. El-Hawary, "Optimal capacitor placement and sizing in unbalanced distribution systems with harmonics consideration using particle swarm optimization," *IEEE Transactions on Power Delivery*, vol. 25, no. 3, pp. 1734–1741, 2010.

[7] C.-F. Chang, "Reconfiguration and capacitor placement for loss reduction of distribution systems by ant colony search algorithm," *IEEE Transactions on Power Systems*, vol. 23, no. 4, pp. 1747–1755, 2008.

[8] S.-J. Huang and X.-Z. Liu, "A plant growth-based optimization approach applied to capacitor placement in power systems," *IEEE Transactions on Power Systems*, vol. 27, no. 4, pp. 2138–2145, 2012.

[9] S. Ganguly, N. C. Sahoo, and D. Das, "Multi-objective planning of electrical distribution systems incorporating shunt capacitor banks," in *2011 International Conference on Energy, Automation and Signal*, 2011, pp. 1–6.

[10] N. Krami, M. A. El-Sharkawi, and M. Akherraz, "Pareto multiobjective optimization technique for reactive power planning," in *2008 IEEE Power and Energy Society General Meeting - Conversion and Delivery of Electrical Energy in the 21st Century*, 2008, pp. 1–6.

[11] K. Prakash and M. Sydulu, "Particle swarm optimization based capacitor placement on radial distribution systems," in *2007 IEEE Power Engineering Society General Meeting*, 2007, pp. 1–5.

[12] T. P. M. Mtonga, K. K. Kaberere, and G. K. Irungu, "Optimal shunt capacitors' placement and sizing in radial distribution systems using multiverse optimizer," *IEEE Canadian Journal of Electrical and Computer Engineering*, vol. 44, no. 1, pp. 10–21, 2021.

[13] P. Díaz, M. Pérez-Cisneros, E. Cuevas, O. Camarena, F. A. Fausto Martinez, and A. González, "A swarm approach for improving voltage profiles and reduce power loss on electrical distribution networks," *IEEE Access*, vol. 6, pp. 49 498–49 512, 2018.

[14] J. Cabral Leite, I. Pérez Abril, and M. S. Santos Azevedo, "Capacitor and passive filter placement in distribution systems by nondominated sorting genetic algorithm-ii," *Electric Power Systems Research*, vol. 143, pp. 482–489, 2017. [Online]. Available: https://www.sciencedirect.com/science/article/pii/S0378779616304230

[15] J. H. Onaka, U. H. Bezerra, M. E. Tostes, and Áthila S. Lima, "A posteriori decision analysis based on resonance index and nsga-ii applied to the capacitor banks placement problem," *Electric Power Systems Research*, vol. 151, pp. 296–307, 2017. [Online]. Available: https://www.sciencedirect.com/science/article/pii/S0378779617302481

[16] A. Jafari, H. Ganjeh Ganjehlou, T. Khalili, B. Mohammadi-Ivatloo, A. Bidram, and P. Siano, "A two-loop hybrid method for optimal placement and scheduling of switched capacitors in distribution networks," *IEEE Access*, vol. 8, pp. 38 892–38 906, 2020.

[17] S. Gupta, V. K. Yadav, and M. Singh, "Optimal allocation of capacitors in radial distribution networks using shannon's entropy," *IEEE Transactions on Power Delivery*, vol. 37, no. 3, pp. 2245–2255, 2022.

[18] L. A. Gallego, J. M. López-Lezama, and O. G. Carmona, "A mixed-integer linear programming model for simultaneous optimal reconfiguration and optimal placement of capacitor banks in distribution networks," *IEEE Access*, vol. 10, pp. 52 655–52 673, 2022.

[19] E. A. Almabsout, R. A. El-Sehiemy, O. N. U. An, and O. Bayat, "A hybrid local search-genetic algorithm for simultaneous placement of dg units and shunt capacitors in radial distribution systems," *IEEE Access*, vol. 8, pp. 54 465–54 481, 2020.

[20] A. Águila, L. Ortiz, R. Orizondo, and G. López, "Optimal location and dimensioning of capacitors in microgrids using a multicriteria decision algorithm," *Heliyon*, vol. 7, no. 9, p. e08061, 2021. [Online]. Available: https://www.sciencedirect.com/science/article/pii/S2405844021021642

[21] L. A. Gallego, J. M. López-Lezama, and O. G. Carmona, "A mixed-integer linear programming model for simultaneous optimal reconfiguration and optimal placement of capacitor banks in distribution networks," *IEEE Access*, vol. 10, pp. 52 655–52 673, 2022.

[22] J. M. Home-Ortiz, R. Vargas, L. H. Macedo, and R. Romero, "Joint reconfiguration of feeders and allocation of capacitor banks in radial distribution systems considering voltage-dependent models," *International Journal of Electrical Power & Energy Systems*, vol. 107, pp. 298–310, 2019. [Online]. Available: https://www.sciencedirect.com/science/article/pii/S0142061518322087

[23] E. A. Almabsout, R. A. El-Sehiemy, O. N. U. An, and O. Bayat, "A hybrid local search-genetic algorithm for simultaneous placement of dg units and shunt capacitors in radial distribution systems," *IEEE Access*, vol. 8, pp. 54 465–54 481, 2020.

[24] S. Das, D. Das, and A. Patra, "Operation of distribution network with optimal placement and sizing of dispatchable dgs and shunt capacitors," *Renewable and Sustainable Energy Reviews*, vol. 113, p. 109219, 2019. [Online]. Available: https://www.sciencedirect.com/science/article/pii/S1364032119304198

[25] T. P. Nguyen, T. A. Nguyen, T. V.-H. Phan, and D. N. Vo, "A comprehensive analysis for multi-objective distributed generations and capacitor banks placement in radial distribution networks using hybrid neural network algorithm," *Knowledge-Based Systems*, vol. 231, p. 107387, 2021. [Online]. Available: https://www.sciencedirect.com/science/article/pii/S0950705121006493

[26] S. F. Santos, D. Z. Fitiwi, M. Shafie-Khah, A. W. Bizuayehu, C. M. P. Cabrita, and J. P. S. Catalão, "New multistage and stochastic mathematical model for maximizing res hosting capacity—part i: Problem formulation," *IEEE Transactions on Sustainable Energy*, vol. 8, no. 1, pp. 304–319, 2017.

[27] A. Jafari, H. Ganjeh Ganjehlou, T. Khalili, B. Mohammadi-Ivatloo, A. Bidram, and P. Siano, "A two-loop hybrid method for optimal placement and scheduling of switched capacitors in distribution networks," *IEEE Access*, vol. 8, pp. 38 892–38 906, 2020.

[28] A. Noori, Y. Zhang, N. Nouri, and M. Hajivand, "Multi-objective optimal placement and sizing of distribution static compensator in radial distribution networks with variable residential, commercial and industrial demands considering reliability," *IEEE Access*, vol. 9, pp. 46 911–46 926, 2021.

[29] M. Babanezhad, S. Arabi Nowdeh, A. Y. Abdelaziz, K. M. AboRas, and H. Kotb, "Reactive power based capacitors allocation in distribution network using mathematical remora optimization algorithm considering operation cost and loading conditions," *Alexandria Engineering Journal*, vol. 61, no. 12, pp. 10 511–10 526, 2022. [Online]. Available: https://www.sciencedirect.com/science/article/pii/S111001682200271X

[30] "Enhanced Load Modeling: Improved Reactive Power Load Modeling," Electric Power Research Institute (EPRI), Tech. Rep. 000000003002022354, August 2021. [Online]. Available: https://www.epri.com/research/programs/108271/results/3002022354

[31] H. Ahmadi, J. R. Martí, and H. W. Dommel, "A framework for volt-var optimization in distribution systems," *IEEE Transactions on Smart Grid*, vol. 6, no. 3, pp. 1473–1483, 2015.

[32] Z. Wang, M. Begovic, and J. Wang, "Analysis of conservation voltage reduction effects based on multistage svr and stochastic process," *IEEE Transactions on Smart Grid*, vol. 5, no. 1, pp. 431–439, 2014.

[33] Z. S. Hossein, A. Khodaei, W. Fan, M. S. Hossan, H. Zheng, S. A. Fard, A. Paaso, and S. Bahramirad, "Conservation voltage reduction and volt-var optimization: Measurement and verification benchmarking," *IEEE Access*, vol. 8, pp. 50 755–50 770, 2020.

[34] M. Diaz-Aguiló, J. Sandraz, R. Macwan, F. de León, D. Czarkowski, C. Comack, and D. Wang, "Field-validated load model for the analysis of cvr in distribution secondary networks: Energy conservation," *IEEE Transactions on Power Delivery*, vol. 28, no. 4, pp. 2428–2436, 2013.

[35] H. Gong, E. S. Jones, and D. M. Ionel, "An aggregated and equivalent home model for power system studies with examples of building insulation and hvac control improvements," in *2020 IEEE Power & Energy Society General Meeting (PESGM)*, 2020, pp. 1–4.

[36] H. Gong, E. S. Jones, A. H. M. Jakaria, A. Huque, A. Renjit, and D. M. Ionel, "Large-scale modeling and dr control of electric water heaters with energy star and CTA-2045 control types in distribution power systems," *IEEE Transactions on Industry Applications*, vol. 58, no. 4, pp. 5136–5147, 2022.

[37] E. S. Jones, R. E. Alden, H. Gong, A. G. Frye, D. Colliver, and D. M. Ionel, "The effect of high efficiency building technologies and PV generation on the energy profiles for typical US residences," in *2020 9th International Conference on Renewable Energy Research and Application (ICRERA)*, 2020, pp. 471–476.

[38] H. Gong, E. S. Jones, R. E. Alden, A. G. Frye, D. Colliver, and D. M. Ionel, "Virtual power plant control for large residential communities using hvac systems for energy storage," *IEEE Transactions on Industry Applications*, vol. 58, no. 1, pp. 622–633, 2022.

[39] H. Gong, E. S. Jones, A. H. M. Jakaria, A. Huque, A. Renjit, and D. M. Ionel, "Generalized energy storage model-in-the-loop suitable for energy

star and CTA-2045 control types," in *2021 IEEE Energy Conversion Congress and Exposition (ECCE)*, 2021, pp. 814–818.
[40] R. Storn and K. Price, "Differential Evolution - A Simple and Efficient Heuristic for Global Optimization over Continuous Spaces," *Journal of Global Optimization*, vol. 11, no. 4, pp. 341–359, 1997. [Online]. Available: http://link.springer.com/10.1023/A:1008202821328
[41] K. Deb, A. Pratap, S. Agarwal, and T. Meyarivan, "A fast and elitist multiobjective genetic algorithm: NSGA-II," *IEEE Transactions on Evolutionary Computation*, vol. 6, no. 2, pp. 182–197, 2002.
[42] A. Ibrahim, S. Rahnamayan, M. V. Martin, and K. Deb, "EliteNSGA-III: An improved evolutionary many-objective optimization algorithm," in *2016 IEEE Congress on Evolutionary Computation (CEC)*, 2016, pp. 973–982.
[43] I. Das and J. E. Dennis, "Normal-boundary intersection: A new method for generating the pareto surface in nonlinear multicriteria optimization problems," *SIAM Journal on Optimization*, vol. 8, no. 3, pp. 631–657, 1998. [Online]. Available: https://doi.org/10.1137/S1052623496307510
[44] J. Blank and K. Deb, "pymoo: Multi-objective optimization in python," *IEEE Access*, vol. 8, pp. 89 497–89 509, 2020.

EVAN S. JONES (Graduate Student Member, IEEE) is a Ph.D. student and a GAANN Graduate Fellow in the SPARK Laboratory at the University of Kentucky (UK), Lexington, KY, USA. He received two B.S. degrees in electrical engineering and computer engineering with a minor in computer science, and an undergraduate certificate for studies in power and energy from UK in 2019. He has also served as the vice president for the joint student chapter of IEEE PES and IAS at UK. In 2020, he was awarded a multi-year GAANN Ph.D. Fellowship administered by the U.S. Department of Education. His research focuses on building energy models (BEMs), distributed energy resources (DERs), virtual power plants (VPPs), and optimal planning and control of electric power systems.

NICHOLAS JEWELL (S'07–M'15–SM'18) received his Doctor of Philosophy degree in electrical engineering from the University of Louisville, Louisville, KY, USA, in 2014. He is currently the Group Leader of Electric Distribution Emerging Technologies Engineering with the Electrical Engineering and Planning Department at Louisville Gas and Electric and Kentucky Utilities (LG&E and KU), part of the PPL Corporation family of companies. At LG&E and KU, he leads a team of engineers to implement cutting edge technologies and manage distributed resource interconnection, while serving as the company subject matter expert in areas such as distribution planning, power systems analysis, and distributed energy resources (DER).

Dr. Jewell's primary focus is on implementing advanced DER strategies and defining and executing a multi-year strategic roadmap pertaining to distribution hosting capacity, distribution system interconnection requirements, customer usage behavior, and system analysis regarding DER impacts to protection systems. He has been an author or co-author for numerous industry publications, has received several Tech Transfer Awards from the Electric Power Research Institute, and has one patent disclosure. Additionally, he was named a Top Innovator by Public Utilities Fortnightly in 2018 for his work with energy storage technologies. Dr. Jewell is also a licensed Professional Engineer in KY and a registered Project Management Professional (PMP).

YUAN LIAO (S'98-M'00-SM'05) is currently a Professor holding the endowed Blazie Family professorship with the Department of Electrical and Computer Engineering at the University of Kentucky, Lexington, KY, USA.

He is the Director of the Graduate Certificate programs at the Power and Energy Institute of Kentucky. He worked as a consulting R&D engineer and then principal consulting R&D engineer at the Corporate Research Center of ABB Inc., Raleigh, North Carolina from 2000 to 2005. He received his bachelor's degree and master's degree from Xi'an Jiaotong University, second master's degree from National University of Singapore, and PhD degree from Texas A&M University, College Station. His research interests include power system protection, analysis and planning, smart grid, and renewable energy integration.

DAN M. IONEL (M'91–SM'01–F'13) received the M.Eng. and Ph.D. degrees in electrical engineering from the Polytechnic University of Bucharest, Bucharest, Romania. His doctoral program included a Leverhulme Visiting Fellowship with the University of Bath, Bath, U.K and he later was a Postdoctoral Researcher with the SPEED Laboratory, University of Glasgow, Glasgow, U.K.

Dr. Ionel is a professor of electrical engineering and the L. Stanley Pigman Chair in Power with the University of Kentucky, Lexington, KY, USA, where he is also the Director of the Power and Energy Institute of Kentucky and of the SPARK Laboratory. He previously worked in industry for more than 20 years. Dr. Ionel's current research group projects on smart grid and buildings, and integration of distributed renewable energy resources and energy storage in the electric power systems are sponsored by NSF, DOE, industry and utilities. He published more than 200 technical papers, including some that received IEEE awards, was granted more than 30 patents, and is co-author and co-editor of the book "Renewable Energy Devices and Systems – Simulations with MATLAB and ANSYS", CRC Press.

Dr. Ionel received the IEEE PES Veinott Award, was the Inaugural Chair of the IEEE IAS Renewable and Sustainable Energy Conversion Systems Committee, an Editor for the IEEE TRANSACTIONS ON SUSTAINABLE ENERGY, and the Technical Program Chair for IEEE ECCE 2016. He was the Editor in-Chief for the Electric Power Components and Systems Journal and is currently the Chair of the Steering Committee for IEEE IEMDC.